BIOCHEMISTRY
including biophysical chemistry & molecular biology
Article

Biochemistry **2009,** *48,* 11441–11448 11441
DOI: 10.1021/bi901017y

Orientational Landscapes of Peptides in Membranes: Prediction of ^{2}H NMR Couplings in a Dynamic Context†

Santi Esteban-Martín,‡ Diana Giménez,‡ Gustavo Fuertes,‡ and Jesús Salgado*,‡,§

‡*Instituto de Ciencia Molecular, Universitat de València, Polígono La Coma s/n, 46980 Paterna, Valencia, Spain, and*
§*Departamento de Bioquímica y Biología Molecular, Universitat de València, C/Dr. Moliner, 50, 46100 Burjassot, Valencia, Spain*

Received July 9, 2009; Revised Manuscript Received October 20, 2009

ABSTRACT: Unlike soluble proteins, membrane polypeptides face an anisotropic milieu. This imposes restraints on their orientation and provides a reference that makes structure prediction tractable by minimalistic thermodynamic models. Here we use this framework to build orientational distributions of monomeric membrane-bound peptides and to predict their expected solid-state ^{2}H NMR quadrupolar couplings when labeled at specific side chain positions. Using a complete rigid-body sampling of configurations relative to an implicit lipid membrane, peptide free energy landscapes are calculated. This allows us to obtain probability distributions of the peptide tilt, azimuthal rotation, and depth of membrane insertion. The orientational distributions are broad and originate from an interplay among the three relevant rigid-body degrees of freedom, which allows population of multiple states in shallow free energy minima. Remarkably, only when the orientational distributions are taken into account do we obtain a close correlation between predicted ^{2}H NMR splittings and values measured in experiments. Such a good correlation is not seen with splittings calculated from single configurations, being either the averaged or the lowest free energy state, showing there are distributions, rather than single structures, that best define the peptide−membrane systems. Moreover, we propose that these distributions contribute to the understanding of the rigid-body dynamics of the system.

The global positioning of a membrane protein with respect to the planar lipid bilayer is of great functional significance, as it determines the protein−membrane binding mode and helps in definition of mechanisms of action (*1*−*4*). Such a relative placement is given by the molecular orientation of the protein with respect to the membrane plane and its depth of insertion in the lipid bilayer (Figure 1). For large proteins in a membrane-bound state, a direct and precise measure of these structural parameters is technically challenging and seldom performed (see refs *1* and *4*−*6* as examples). However, for simple membrane-active peptides and fragments of membrane proteins, detailed molecular positioning is investigated extensively using spectroscopic methods, like NMR (*2*, *7*−*12*), FTIR (*3*, *13*), CD (*14*, *15*), fluorescence spectroscopy (*16*), and EPR (*17*).

In principle, the equilibrium state of peptide molecules or protein fragments within a membrane can be predicted to low resolution by taking into account simply a measure of their relative preference for the hydrophobic bilayer versus the bulk water solvent. For example, hydrophobicity scales of amino acid residues allow one to search for putative transmembrane (TM)[1] segments from target proteins (*18*−*22*). Some of these scales are made of partition free energies of amino acid residues between water and several organic solvents mimicking the hydrophobic core of the lipid bilayer (*23*−*25*). However, partitioning of residues to the membrane is a function of the position along the normal axis, reflecting large gradients in polarity, hydration, density of specific chemical groups, and fluidity across the membrane. As this was recognized, an interfacial scale was introduced and measured experimentally for palmitoyloleoylphosphatidylcholine (POPC) (*26*). In a more sophisticated manner, this complexity has recently been recalled in a biological context, where the translocon membrane insertion machinery in an in vitro translation system is deployed to determine per residue free energies that are found to depend on the relative position along the nascent TM helix (*27*). These experimental free energies suffer from low spatial resolution but can in principle be complemented by detailed molecular simulation techniques. Potentials of mean force resolved along the membrane normal have been derived from experimental membrane protein structures (*28*, *29*) and by umbrella sampling molecular dynamics simulations of amino acid side chain analogues at full atomic detail (*30*, *31*). Additionally, implicit membrane systems have been developed using different continuum models (*32*−*36*). From a different perspective, the adequacy between peptides and membranes is often rationalized within the concept of hydrophobic mismatch (*37*, *38*). This, in its most simplified geometric version, allows prediction of the slant angle of peptides, since adjusting the tilt is an easy way for these molecules to achieve an optimal overlap between its hydrophobic length and the membrane hydrophobic thickness. Some elaborated extensions of these ideas have recently been employed to search within configurational energy landscapes for the relative position within the

†This work was supported by a grant from the Spanish Ministerio de Ciencia e Innovación, MICINN (BFU2007-67097/BMC), financed in part by the European Regional Development Fund (ERDF). S.E.-M. thanks MICINN for a FPU fellowship, and G.F. thanks the University of Valencia for a V Segles Fellowship.

*To whom correspondence should be addressed: Instituto de Ciencia Molecular, Universitat de València, Polígono La Coma s/n, 46980 Paterna, Valencia, Spain. Telephone: +34963543016. Fax: +34963543273. E-mail: jesus.salgado@uv.es.

[1]Abbreviations: TM, transmembrane; POPC, palmitoyloleoylphosphatidylcholine; MD, molecular dynamics; WW, Wimley and White; DMPC, dimyristoylphosphatidylcholine; DOPC, dioleylphosphatidylcholine; 3D, three-dimensional; GALA, geometric analysis of labeled alanines; rmsd, root-mean-square deviation.

Published on Web 10/27/2009

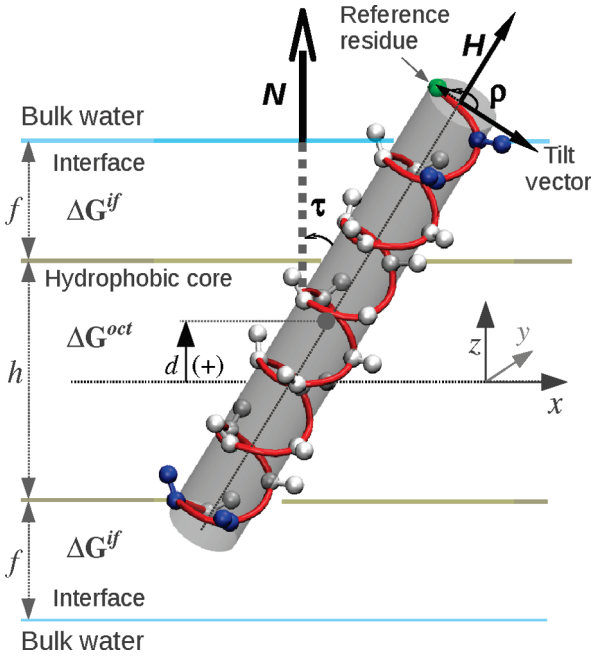

FIGURE 1: Relative placement of a helical peptide in a lipid bilayer. The peptide position is defined by its depth of insertion, *d*, and a pair of orientational angles, tilt (τ) and the azimuthal rotation (ρ). Being the membrane normal (**N**) aligned with the *z*-axis, the distance *d* is the *z* coordinate of the peptide center of mass, with a $z = 0$ set arbitrarily at the center of the lipid bilayer. τ is the angle formed between the molecular long helix axis (**H**, from the C-terminus to the N-terminus) and the membrane normal. ρ is the angle between the direction of the peptide tilt and a vector perpendicular to **H** pointing to the C^{α} carbon of a reference residue (here the first residue). The peptide is represented by the backbone atoms with an α-helix structure, plus C^{β} atoms. The N-terminus is at the top, with the first residue colored green. The atoms colored blue represent flanking residues, like Lys and Trp in KALP/KLP and WALP/WLP peptides. The membrane is represented implicitly as regions defined by widths *h* (hydrophobic core), to which we apply partition free energies from the WW octanol scale (ΔG^{oct}), and *f* (interface), characterized by partition free energies from the WW POPC−interface scale (ΔG^{if}).

bilayer and the expected (most stable) orientation of membrane proteins (*28*, *32*, *34*, *39*−*41*).

However, more than precise positions and orientations, a complete understanding of protein− or peptide−membrane complexes should include knowledge of the frequency distributions of these structural parameters. In fact, in the partially disordered and highly dynamic lipid matrices, large molecular fluctuations of monomeric peptides and protein fragments can be expected. Recent studies based on molecular dynamics (MD) simulations have proposed that such information is important for the interpretation of solid-state NMR experiments, since fast orientational fluctuations (*42*) can average the NMR parameters (*43*−*46*). Supporting this view, we have shown that previously reported ^{2}H NMR data can indeed be reinterpreted with better quality of the fits by introduction of peptide dynamics in the form of Gaussian fluctuations of the orientation angles (*47*). Notably, this alternative analysis yields estimates of the amplitudes of the peptide rigid-body movements (standard deviations of the tilt and azimuthal rotation), typically at the expense of different fitted (mean) tilt angles (*47*). While this has opened a new window for the structural investigation of the peptide−membrane systems, some important questions regarding the specific mode of peptide rotational movement and mechanisms of fluctuation remain. Furthermore, the proposed dynamic analysis is still not free from uncertainty, since best fit values fall often in shallow minima of the error functions (*47*). Such questions can again be addressed by simulation methods, like atomistic MD, that allow one to build an explicit dynamic molecular model from which one can calculate directly the expected experimental measures (*43*, *44*, *46*, *48*). However, compared to the small time windows that can be accessed by simulations at atomic detail (*49*), membrane−peptide reorientation is a slow relaxing process (*42*) that in practice limits the possibilities of studies using these methods.

Here we calculate complete rigid-body landscapes based on the relative stability of membrane peptides with respect to their tilt, azimuthal rotation, and insertion depth in the bilayer. This strategy is applied to a number of monomeric peptide systems previously investigated by ^{2}H solid-state NMR experiments, including the WALP/WLP and KALP/KLP model TM peptides (*7*, *47*, *50*, *51*), and the amphipathic antimicrobial peptide PGLa (*2*, *15*, *52*, *53*). To calculate peptide free energies, we model the membrane implicitly considering both the hydrophobic and polar regions by applying experimental whole-residue values from the double scale of partition free energies of Wimley and White (WW) (*23*, *26*, *54*). Broad probability distributions for the tilt and azimuthal rotation angles are obtained, suggesting that extensive rigid-body dynamics is an intrinsic property of monomeric membrane−peptide systems, as proposed from NMR relaxation studies (*42*, *55*). The free energy-based configurations are further used to simulate directly solid-state ^{2}H NMR splittings, which compare well with values measured in experiments. Thus, avoiding the limitations of experimental interpretations under conditions of dynamics (*47*), this study illustrates the predicting value of a relatively simple approach and its capacity to evaluate, at very low computational cost, peptide orientation and dynamics.

METHODS

Models of Peptide Systems. Structure coordinates in Protein Data Bank (PDB) format for the WALP23, WLP23, KALP23, KLP23, and PGLa peptides were generated as ideal uniform α-helices with the help of the Swiss PDB Viewer (http://www.expasy.org/spdbv) (*56*). To imitate the synthetic peptides used in the corresponding experimental studies, in all cases the C-terminus was amidated and the N-terminus acetylated, except for the antimicrobial peptide PGLa, for which the N-terminus was kept as a charged amino group.

Definition of the Position and Orientation of Peptides in Membranes. The relative placement of a rodlike α-helical peptide in a lipid membrane is defined by a set of three parameters, *d*, τ, and ρ (Figure 1). The parameter *d* defines the peptide position as the depth of insertion in the membrane and corresponds to the distance between the peptide center of mass and the midplane of the bilayer. The angles τ and ρ express the peptide orientation and correspond to the tilt of the peptide principal axis vector (**H**, defined from the C-terminus to the N-terminus) with regard to the membrane normal vector (**N**) and its azimuthal rotation about the latter principal axis, respectively. For the α-helix, **H** is determined through diagonalization of the inertia tensor corresponding to the backbone heavy atoms. Then, ρ is found in the plane perpendicular to **H**, as the angle between a vector pointing in the direction of the tilt, calculated as $\mathbf{H} \times (\mathbf{H} \times \mathbf{N})$, and a reference vector pointing into the C^{α} atom of an arbitrary residue [here the first residue (see Figure 1)].

Construction of the Configurational Space and Calculation of Peptide Free Energies. Configurations were defined

depending on the relative placement of each considered peptide, treated as a monomer, with respect to the membrane, given by variable $\{d,\tau,\rho\}$ sets of parameters for a constant peptide structure (rigid-body assumption) taken as a canonical α-helix. If the membrane midplane is set to coincide with the $x-y$ plane of the coordinate system, d (aligned with the normal **N**) coincides with the z coordinate, and the membrane is represented implicitly as the region of space between $z = -(f + h/2)$ and $z = (f + h/2)$, where h and f are values of thickness for the hydrophobic and interface regions, respectively. We have used an f of 5 Å (*57*) and values of h taken from the literature (*58*, *59*): 25.4 and 27.1 Å for dimyristoylphosphatidylcholine (DMPC) and dioleylphosphatidylcholine (DOPC), respectively. Alternative values of h, like those determined from lipid tail segmental order parameters in ^{2}H NMR measurements (*60*, *61*), were seen to affect the mean values of the tilt angle up to a maximum of 5°, while leaving the mean of the azimuthal rotation angle and the width of tilt and rotation distributions almost unaffected. On the other hand, errors in the f value would have the main consequence of increasing the degree of broadening of the rotational angle distribution, and thus affect the calculated deuterium splittings. However, as we discuss below, the method seems already to overestimate the width of distributions (seen as an underestimation of the splittings), and variable f and h values would just lead to worse results.

Full configurational landscapes were sampled by translating the peptide along the membrane normal from a d of −50 Å to a d of 50 Å in 0.5 Å steps (a d of 0 Å corresponds to the membrane center) and rotating it at each step through all τ and ρ angles in steps of 1°. For each peptide configuration, the free energy is calculated as the sum of free energies corresponding to each residue, depending on their position in either the membrane hydrophobic core, the membrane interface, or the bulk water. Such relevant residue positions are taken as the z coordinates of the C^β atoms. Other options are possible, like C^α or the center of mass of the residue; however, the C^β atom has the advantage of being attached rigidly to the helix structure, while being independent of the configuration of the side chains (which for the cases studied is unknown). Additionally, it captures the end-to-end asymmetry of the helical peptide, as the $C^\alpha-C^\beta$ bond points toward the N-terminus (Figure 1). Then, the appropriate free energy values for each residue are extracted from the empirical whole-residue scales (side chain plus peptide bond) of Wimley and White. These contain free energies of transfer from water to the POPC bilayer interface (*26*), which we use to map residues at the membrane interface, or from water to *n*-octanol (*23*), used for residues falling in the membrane acyl chain region. We also considered partition free energies for the N-terminal and C-terminal groups (*54*). Additionally, we use a per-residue correction of −0.4 kcal/mol to account for peptide folding in the membrane, corresponding to hydrogen bonding of the amide NH and CO groups in α-helices. This value has been determined for the coil to helix transition of melittin in membranes, and it is in principle justified at least for values of the interface scale (*62*). Here we apply it also to the octanol scale since a similar correction has been calculated for the folding of α-helices in different alcohols (*63*).

The calculated free energies were converted into probabilities as

$$P(d,\tau,\rho) = e^{-[\Delta G(d,\tau,\rho)/RT]} \quad (1)$$

where R is the gas constant and T the absolute temperature (taken to be 303 K).

Calculation of Expected ^{2}H NMR Quadrupolar Splittings. Virtual (experiment-like) ^{2}H splittings that would correspond to the orientation of $C_\alpha-C_\beta$ bonds of labeled residues in our configuration space were back-calculated using the strategy explained in a previous MD study (*43*). Briefly, we consider virtual CD_3-labeled Ala residues at the same sequence positions as those used for experiments. Assuming that the membrane normal is aligned with the magnetic field, instantaneous static splittings ($\Delta\nu_{ins}$) are back-calculated for each virtual labeled residue, in each particular state of the full configurational space, as

$$\Delta\nu_{ins} = 3/4(e^2Qq/h)(3\cos^2\theta - 1) \quad (2)$$

where e^2Qq/h is the nuclear quadrupole coupling constant, taken to be 168.0 kHz for a CD group (*50*, *51*), and θ is the orientation of the $C_\alpha-C_\beta$ bond (the $C_\alpha-C_\beta D_3$ vector) with respect to the membrane normal. The $\Delta\nu_{ins}$ values are then multiplied by $^1/_3$ to account for fast motional averaging about the $C_\alpha-C_\beta D_3$ bond in the virtual CD_3 splittings. For the complete configurational space, weighted average splittings ($\Delta\nu_{aver}$) were calculated for each labeled position, considering the probability of each sampled state as given by eq 1. Splittings were also obtained for the minimum free energy state and for the state defined by the weighted average values of d, τ, and ρ.

RESULTS AND DISCUSSION

How Do Membrane Peptides Orient, and Why Does Their Orientation Fluctuate? Similar to the membrane lipids, the membrane-bound peptides are amphipathic and tend to accommodate the different residues along their sequence, depending on their physicochemical properties, in the bilayer hydrophobic core, the interface, or the bulk water. The position and orientation finally acquired can be rationalized as a global optimization considering the partition free energy of each individual residue. In our model, we have sampled all possible configurations depending on three main rigid-body degrees of freedom of the peptide and divided the available peptide environment into three clearly defined regions that are represented by distinct free energy values for each residue (see Figure 1 and Methods). The different peptide states are then represented by sets of $\{d,\tau,\rho\}$ parameters, each one labeled by their partition free energy (or by their probability). The global configurational landscape exhibits an absolute minimum energy (maximum probability) for a triad of values $\{d^{min},\tau^{min},\rho^{min}\}$. However, other low-energy configurations are possible, as we can appreciate through stability-based probability distributions. For illustrative purposes, such distributions are represented in three-dimensional (3D) plots of pairs $\{\tau,d\}$, $\{\rho,d\}$, and $\{\tau,\rho\}$ mapped to their respective probabilities, shown in Figure 2 for WLP23, KLP23, and PGLa in an implicit DMPC membrane. Alternatively, two-dimensional distributions can be drawn for each of the three parameters [corresponding to projections of the 3D plots (see Figure S1 of the Supporting Information)]. The average values for each peptide−membrane system studied are collected in Table 1. The broadness of the 3D distributions shows that the most probable states reside in shallow free energy minima. This is due to the fact that variations of the three degrees of freedom provide multiple ways of changing the relative position of residues, particularly near the interface, which may end up partially compensating each other in terms of the total peptide free energy. For example, by sampling small τ values, KLP23 can easily exchange between the complete range of ρ values (Figure 2D), which produces a very broad ρ peak [compare this

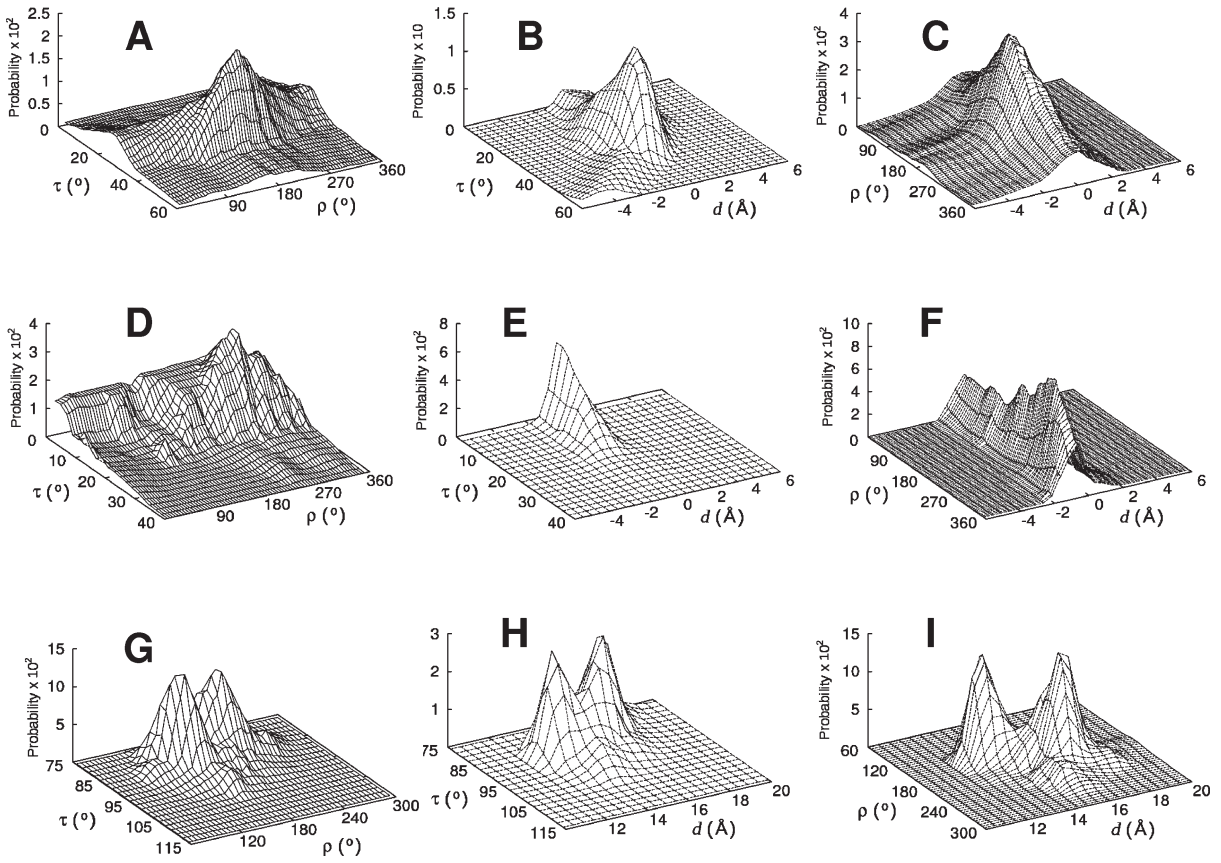

FIGURE 2: Probability surfaces for states of peptides WALP23 (A−C), KALP23 (D−F), and PGLa (G−I) in an implicit DMPC membrane. The probabilities are calculated using eq 1 from the corresponding free energies. Each pair of variables, $\{\tau,\rho\}$ (A, D, and G), $\{\tau,d\}$ (B, E, and H), and $\{\rho,d\}$ (C, F, and I), is mapped to the accumulated probability for all states given by the third variable (d for panels A, D, and G, ρ for panels B, E, and H, and τ for panels C, F, and I).

Table 1: Summary of Systems Studied and Comparison of Orientational Parameters Obtained from Our Model with Those Determined from MD Simulations and from Experimental NMR Data

							from experiments			
		from partition free energies[b]			from atomistic MD simulations[c]		fits without explicit dynamics[d]		fits with explicit dynamics[e]	
peptide	lipid[a]	d (Å)	τ (deg)	ρ (deg)	τ (deg)	ρ (deg)	τ (deg)	ρ (deg)	τ (deg)	ρ (deg)
WLP23	DMPC	−1.0 ± 2.0	34 ± 15	180 ± 88	31 ± 12	173 ± 58	8	176	−;	−;
	DOPC	−1.0 ± 2.3	28 ± 16	179 ± 89	−;	−;	5	179	−;	−;
WALP23	DMPC	−1.0 ± 3.5	36 ± 19	178 ± 94	33 ± 12	153 ± 91	6	158	14 ± 15[f]	158 ± 71[f]
	DOPC	−1.0 ± 3.5	30 ± 19	178 ± 94	−;	−;	4	154	11 ± 18[f]	154 ± 68[f]
KLP23	DMPC	−0.5 ± 1.0	11 ± 10	275 ± 92	20 ± 11	206 ± 104	8	265	−;	−;
	DOPC	−0.5 ± 1.0	10 ± 8	313 ± 88	−;	−;	6	265	−;	−;
KALP23	DMPC	−0.5 ± 2.0	11 ± 11	277 ± 88	∼22 ± 10	−;	8	281	−;	−;
	DOPC	−0.5 ± 1.3	10 ± 8	314 ± 91	−;	−;	5	273	−;	−;
PGLa (S state)	DMPC	15.0 ± 2.8	86 ± 10	181 ± 58	−;	−;	82	175	82 ± 17	175 ± 15
PGLa (T state)	DMPC						54	171	55 ± 11	171 ± 15

[a]The membrane is modeled implicitly, with a hydrophobic thickness of 25.4 Å for DMPC and 27.1 Å for DOPC, and an interface thickness of 5 Å in both cases. [b]From this work. Averages from distributions ± standard deviations. [c]From refs *43* (WLP23 and KLP23), *44* (WALP23), and *65* (KALP23). Averages from distributions ± standard deviations. [d]For all systems, the experimental orientation was determined from ^{2}H NMR quadrupolar splittings. For WALP/WLP and KALP/KLP peptides, the values are those from refs *7* and *50* determined using a quasi-static version of the GALA method (S = 0.88). For PGLa, the values are from data in ref *52*, using a fitted order parameter ($0 \le S \le 1$) as a way to account implicitly for peptide dynamics. Since in this latter case the definition of angles in the original experimental studies is different from our definition, we have recalculated such angles using the reported experimental ^{2}H NMR data and according to our definition (see Methods). [e]Taken from ref *47*, except for the values for WALP23 in DOPC which are calculated here as explained in ref *47*. Missing values correspond to cases with an insufficient number of measured ^{2}H NMR splittings to allow the explicit-dynamics GALA fits. [f]Best fit values fall in shallow minima of the error function (*47*). A wide range of angles and associated Gaussian distributions for the tilt and azimuthal rotations (see the text) cannot be distinguished within experimental error (∼1−2 kHz).

case with WLP23 (Figure 2A)]. Such relative redundancy of structural changes occurs especially for peptides in a TM state and for variations of the azimuthal rotation, thus giving in these cases broad distributions for the τ dimension and very broad distributions (with non-zero probability for all angles) for the ρ dimension (Figure 2A−F; see also Figure S1 of the Supporting Information).

In our coarse grained peptide−implicit membrane systems, anchoring is achieved exclusively depending on the preference of residues near the hydrocarbon to interface transition (and to a smaller extent near the interface to water transition) for either of these regions, as dictated by their respective partition free energy values. In such a model, the lack of specific interactions at fixed positions between the peptide side chains and the lipid headgroups might be seen as promoting wider distributions. However, in real membranes, the interacting groups from the lipids also fluctuate in position, effectively widening the orientation distributions of membrane-bound peptides. In agreement with these ideas, distributions similar to the ones reported here were also obtained from all-atom MD simulations (*43*, *44*). We should also note that the distributions reported here apply to only monomeric peptides, which for the cases studied is supported by experiments (*2*, *64*).

The tilts of W-flanked TM peptides are smaller in thicker membranes (27.1 Å, in DOPC) than in thinner membranes (25.4 Å, in DMPC), as expected from a smaller hydrophobic mismatch in the former (see Table 1 and Figure S1B of the Supporting Information). On the other hand, the K-flanked peptides show clearly smaller tilts than the W-flanked peptides for the same membrane thickness, as it corresponds to a contribution of Trp residues to the peptide hydrophobic length. In fact, the two K-flanked peptides appear to reach near hydrophobic matching conditions already for DMPC (Table 1), since the average tilt reaches the proposed minimum tilt value (∼10°) (*65*) and keeps almost the same for the thicker implicit DOPC membrane. The azimuthal rotation angle distributions are not very sensitive to the membrane width or the nature of the peptide core (either L-based or AL-based) but depend on the type of flanking residue (see averaged values in Table 1). Although Trp or Lys is located at the same angular position about the helix axes in the respective peptides, the different partition free energies of these residues translate into the selection of clearly different ρ angles. Thus, KLP23 and KALP23 prefer mean ρ angles near 300°, which better accommodates the polar Lys at the interface, while the tendency of Trp toward the apolar core gives a preferred average ρ of ∼180° for WLP23 and WALP23. Nevertheless, the large width of the ρ distributions shows that the peptide rotation is only weakly constrained, which predicts strong dynamics for these systems.

In contrast to the orientation angles, the distance of membrane insertion is a well-defined parameter. For the TM model systems, the peaks are placed around the center of the membrane, with an approximate symmetry reflecting the relative end-to-end symmetry of the peptide sequences (Figure 2B,C,E,F). However, there is a clear tendency for a negative d (Table 1), related to differences in partition free energies from different N- and C-terminal parts (including capping groups) and the fact that the $C_\alpha-C_\beta$ bonds project the side chains toward the N-terminus (Figure 1).

The natural amphipathic peptide PGLa exhibits a behavior clearly different from that of TM peptides. Its free energy-based distributions show a more constrained orientation, with the helix laying almost flat in the membrane and narrower τ and ρ distributions going down to zero probability outside the representative states (Figure 2G−I). In this binding mode, the depth position plays an important role for the adjustment of the peptide to the membrane. The distribution of d indicates that the peptide resides mostly immersed in the hydrophobic slab, although near the membrane interface where the polar residues, especially the charged Lys, can gain access. There, it appears to occupy a broad region with two partially overlapping peaks at d values of ∼13 and ∼16 Å (Figure 2H,I). Both positions are compatible with the same tilt distribution (Figure 2H), although each one selects a different azimuthal rotation distribution (Figure 2I), both placing the Lys residues toward the water phase and corresponding to ρ values of ∼150° and ∼200°, with an average at ∼180° (see also Figure S2 of the Supporting Information). Such a configuration coincides nicely with that found experimentally at a 1:200 peptide:lipid molar ratio (monomeric PGLa, S state) but is clearly distinguishable from that assayed at a 1:50 peptide:lipid molar ratio (dimeric PGLa, T state) (Table 1) (*52*).

From this analysis, we can conclude that monomeric membrane-bound peptides in the two most typical configurations (across the membrane and flat in the membrane interface) are expected to be highly mobile. In what follows, we give a detailed comparison to available ^{2}H NMR experimental data, with direct predictions of ^{2}H splittings, and discuss implications of peptide dynamics for the experimental interpretations.

COMPARISON WITH EXPERIMENTS

Orientation Angles. The orientations of WLP23/WALP23 and KLP23/KALP23 have been extensively studied by ^{2}H NMR (*7*). The literature values were calculated from fits of a model assuming α-helices with limited mobility (fixed order parameter $S = 0.88$, geometric analysis of labeled alanines, GALA), listed in Table 1 (*7*, *51*). For PGLa, the orientation has also been elucidated from ^{2}H NMR experiments, in this case analyzed using a simplified dynamic model that accounts for mobility by fitting an order parameter scaling factor $0 \leq S \leq 1$ (implicit dynamic GALA) (*52*, *53*). We have shown recently that it is possible to perform an alternative analysis of the ^{2}H splittings, in most cases with improved results, by fitting models that consider a mobile rigid helix via Gaussian fluctuations of the tilt and azimuthal rotation (explicit dynamic GALA) (*47*). This analysis was conducted under the assumption of fast axial diffusion and off-axis (wobbling) motions of the peptides (on the ^{2}H NMR time scale) which was based on relaxation studies on similar systems (*42*). The alternative dynamic fits demonstrate that the tilt is particularly model-dependent, especially for TM peptides (small to moderate τ) with vigorous rigid-body mobility. In contrast, the rotation angle ρ is practically independent from the consideration of dynamics in the analysis (*43*, *47*), which means that this structural parameter can be unambiguously determined from experimental ^{2}H splittings. Because the explicit dynamic analysis uses extra adjustable parameters in the fit, a large number of experimental splittings is needed, available only for WALP23 and PGLa. The values obtained from explicit dynamic GALA fits for these latter peptides are also given in Table 1.

As described previously (*47*), in the case of monomeric PGLa, aligned almost flat in the membrane and with small angular fluctuations, there is no variation of the τ and ρ angles if they are determined either using the implicit dynamic or the explicit dynamic GALA analysis. For the case of a low peptide concentration (1:200 peptide:lipid molar ratio, monomeric S state) (*2*, *52*), both experimental angles compare nicely with the corresponding weighted average values from our free energy-based distributions (Table 1). Of note, even a small deviation of τ from a completely flat alignment ($< 10°$), which places the amidated C-terminus in a slightly more inserted position compared to the N-terminal amine group, is predicted by our model.

For TM peptide WALP23, the main effect of including dynamics in the experimental analysis is a substantial increase in τ, now a mean of a Gaussian distribution (*47*). However, the

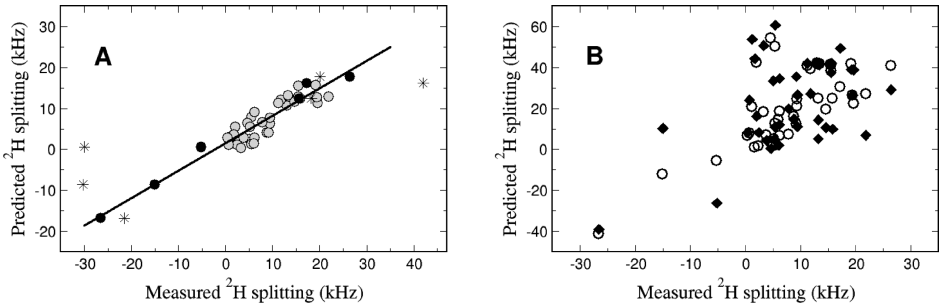

FIGURE 3: Correlation plots between experimental ^{2}H NMR splittings and virtual splittings back-calculated (predicted) from free energy landscapes. Only splittings that were well resolved in experiments are included in the figure. In panel A, the predicted splittings are weighted averages considering the probability of each sampled state from the full configurational space. The black line is a linear fit of points represented as filled circles (black and gray colored). The gray filled circles correspond to data for model transmembrane peptides, for which experimental values are from ^{2}H solid-state NMR measurements of D_3C-Ala-labeled WLP23, KLP23, KALP23 (from ref *7*), and WALP23 (from ref *50*), in membranes of either DMPC or DOPC. For none of these studies is there experimental information about the sign of the splitting (as it is normally the case), and thus, the predicted splittings are taken as absolute values. The black filled circles correspond to data for D_3C-Ala-labeled PGLa in DMPC at a 1:200 peptide:lipid molar ratio (experimental values from ref *52*). In this case, the sign is known from a parallel ^{19}F NMR study (*53*). Stars correspond to data for PGLa in DMPC at 1:50 peptide:lipid molar ratio (*52*) (not used for the linear fit). In panel B, the predicted splittings are values calculated for single states corresponding to either the average state (white circles) or the minimum energy state (black diamonds).

tilts predicted from our partition free energy landscape appear to be larger than the experimental values, even if these latter values are determined using the dynamic GALA fits (Table 1). Nevertheless, we have shown that in the case of highly mobile TM peptides the use of Gaussian distributions of the orientation angles appears still to be insufficient to remove the uncertainty of the extracted tilts, since the best fit values fall in shallow minima of the error functions (*47*). For example, in the case of WALP23, good fits to experimental splittings (rmsd < 1 kHz) can be obtained for mean τ values in a wide range from 8° to 24° in DMPC, and from 4° to 24° in DOPC. In contrast, when experimental ρ angles are compared with results from the partition free energy landscapes, the agreement is generally good (Table 1), especially considering the complexity and large width of the ρ distributions. Note also that in this study the difference between the ρ angles for W-flanked and K-flanked peptides originates exclusively from the free energy values of Trp and Lys (as all the rest is the same for the two types of peptides). This stresses the importance of the flanking residues in determining the ρ structural parameter and supports as well the validity of our strategy, despite the absence of specific interfacial interactions.

^{2}H NMR Splittings. A direct comparison with measured ^{2}H NMR splittings, instead of angles determined from these data, avoids the problems related to limitations of the method chosen for the experimental analysis (*43*, *47*). For that we back-calculated averaged splittings corresponding to our free energy-based distributions, assuming fast reorientational motions of the peptide compared to the ^{2}H NMR scale (*42*, *66*). The comparison is made in a correlation plot using experimental splittings from the literature [for WLP23, WALP23, KLP23, and KALP23 in membranes of either DMPC or DOPC (*7*, *50*) and for PGLa in DMPC (*53*, *52*)] and predicted splittings calculated from the free energy-based distributions (Figure 3). The few negative splittings are from PGLa, for which the sign is know through a parallel ^{19}F NMR study (*53*). For the rest, we represent absolute values.

Notably, for splittings calculated considering the complete configurational space, the correlation with experimental values is very good (Figure 3A, filled circles). The slight underestimation of the predicted splittings might be due to a somewhat overestimated peptide dynamics in our model, probably because of the lack of specific interfacial interactions (mentioned above). In contrast, a poor correlation was found for splittings calculated from single states, being either the minimum free energy state or the averaged state (Figure 3B). This result supports the possibility that it is the complete distribution of position and orientation states that best represents dynamic peptide−membrane systems, instead of unique states. Additionally, it strengthens the importance of considering distributions for the NMR analysis of such systems. Because these are direct comparisons to measured ^{2}H NMR quantities, the correlation in Figure 3A overall indicates that the frequency distributions of positional and orientational parameters, calculated from experimental partition free energies, represent good approximations to the real distributions and are then useful for describing the rigid-body orientation and dynamics of membrane peptides. For example, the predicted ^{2}H splittings in the case of PGLa compare much better with experimental results obtained at a 1:200 peptide:lipid molar ratio [Figure 3A (●)] than at a 1:50 molar ratio [Figure 3A (∗)]. This is also observed in a comparison of the orientation angles (Table 1) and is in agreement with the reported conclusion that the monomeric state of PGLa (as modeled here) corresponds to the case of a low peptide concentration (so-called S state), in contrast to a tilted (T) state, found at a higher concentration and described as a dimer (*2*, *52*).

The orientation and dynamics of model TM peptides with emphasis on the distributions of τ and ρ angles and their implication for NMR experimental analysis has been investigated before by MD studies at atomic resolution (*43*, *44*). For these and other simulations reporting average τ and ρ angles, the values are also given in Table 1. The agreement with values from our stability-based distributions is very good in the case of the two W-flanked peptides, both for the averaged values of τ and ρ and for their standard deviations. With respect to the K-flanked peptides, the widths of distributions also agree well; however, the averaged tilts from the free energy landscapes are clearly smaller than the averages from MD trajectories, and there is a significant offset in the case of ρ [available from only MD for KLP23 in DMPC (*43*)]. Nevertheless, the angles from the free energy analysis agree better with the experimental angles (Table 1), which may indicate insufficient sampling in the case of MD simulations. For the analysis of peptide reorientation, atomistic MD simulations are limited by the time scale available, today on the order of hundreds of nanoseconds, which is still small compared with typical relaxation times of the peptide rotational

motions (*42*, *67*). However, for the free energy-based distributions, the sampling of rigid-body configurations is complete. It is then interesting that such global distributions overlap well with the MD distributions. Similarly, recent coarse-grained MD simulations, where the time limit is easily broken, have shown regular tilt distributions that superimpose with those from a set of comparable atomistic MD runs and compare well with the ones described here (*68*).

Most encouraging is the fact that, despite their particular limitations, both MD (*43*, *44*, *46*, *48*) and the free energy-based analysis reproduce fairly well experimental solid-state NMR parameters, meaning that they both yield good descriptions of, at least, monomeric peptides in membranes. However, compared to the atomistic MD studies, the free energy analysis described in this work has the additional advantage of allowing exploration of a complete orientational space and being easily affordable at a very low computational cost. Such computational simplicity and good prediction capacity make it a good auxiliary method for experimental analysis, at least of ^{2}H NMR data.

CONCLUSIONS

The positional and orientational order of lipids in biological membranes defines a complex environment that conditions the binding mode (relative position and orientation) of membrane peptides and proteins. We have demonstrated that, at least for monomeric peptides, such relative placement obeys simple rules and can be predicted from a global free energy landscape as a function of the tilt, azimuthal rotation, and insertion depth, based on empirical partition free energies of individual amino acid residues. Each of these parameters governs the total peptide free energy in a different manner, although they are coupled to each other. This, and the broad distributions of the tilt and azimuthal rotation, illustrate the dynamic character of these monomeric membrane peptides, for which large rigid-body fluctuations appear to be an intrinsic property (especially for the TM cases).

The comparison with experimental orientation angles is difficult, because of the importance of the distributions, which are unknown in reality, for the experimental analysis. However, a more direct comparison using measured ^{2}H NMR splittings and corresponding virtual values back-calculated from our free energy landscapes shows a very good correlation of both sets of values, provided the complete distributions, rather than single minimum energy or averaged states, are chosen. This stresses the importance of considering dynamics for the NMR experimental analysis and shows that for the case of membrane peptides such dynamics can be predicted using simple and fast approaches. Finally, we have also seen that an optimized placement and orientation makes a clear difference in the relative stability of the protein fragments in membranes. Thus, we can expect that implementing such an optimization in the algorithms used for the prediction of TM fragments should have the capacity to improve their results.

SUPPORTING INFORMATION AVAILABLE

Two figures showing the probability distributions (two-dimensional plots) of the depth of membrane insertion (d), tilt (τ), and azimuthal rotation (ρ) of studied peptides. This material is available free of charge via the Internet at http://pubs.acs.org.

REFERENCES

1. Franzin, C. M., Choi, J., Zhai, D., Reed, J. C., and Marassi, F. M. (2004) Structural studies of apoptosis and ion transport regulatory proteins in membranes. *Magn. Reson. Chem. 42*, 172–179.
2. Glaser, R. W., Sachse, C., Dürr, U. H. N., Wadhwani, P., Afonin, S., Strandberg, E., and Ulrich, A. S. (2005) Concentration-dependent realignment of the antimicrobial peptide PGLa in lipid membranes observed by solid-state ^{19}F-NMR. *Biophys. J. 88*, 3392–3397.
3. García-Sáez, A. J., Coraiola, M., Dalla Serra, M., Mingarro, I., Menestrina, G., and Salgado, J. (2005) Peptides derived from apoptotic Bax and Bid reproduce the poration activity of the parent full-length proteins. *Biophys. J. 88*, 3976–3990.
4. Oh, K. J., Zhan, H., Cui, C., Hideg, K., Collier, R. J., and Hubbell, W. L. (1996) Organization of diphtheria toxin T domain in bilayers: A site-directed spin labeling study. *Science 273*, 810–812.
5. Oh, K. J., Barbuto, S., Meyer, N., Kim, R., Collier, R. J., and Korsmeyer, S. J. (2005) Conformational changes in BID, a pro-apoptotic BCL-2 family member, upon membrane binding. A site-directed spin labeling study. *J. Biol. Chem. 280*, 753–767.
6. Aisenbrey, C., Cusan, M., Lambotte, S., Jasperse, P., Georgescu, J., Harzer, U., and Bechinger, B. (2008) Specific isotope labeling of colicin E1 and B channel domains for membrane topological analysis by oriented solid-state NMR spectroscopy. *ChemBioChem 9*, 944–951.
7. Özdirekcan, S., Rijkers, D. T., Liskamp, R. M., and Killian, J. A. (2005) Influence of flanking residues on tilt and rotation angles of transmembrane peptides in lipid bilayers. A solid-state ^{2}H NMR study. *Biochemistry 44*, 1004–1012.
8. Song, Z., Kovacs, F. A., Wang, J., Denny, J. K., Shekar, S. C., Quine, J. R., and Cross, T. A. (2000) Transmembrane domain of M2 protein from influenza A virus studied by solid-state ^{15}N polarization inversion spin exchange at magic angle NMR. *Biophys. J. 79*, 767–775.
9. Montal, M., and Opella, S. J. (2002) The structure of the M2 channel-lining segment from the nicotinic acetylcholine receptor. *Biochim. Biophys. Acta 1565*, 287–293.
10. Opella, S. J., Marassi, F. M., Gesell, J. J., Valente, A. P., Kim, Y., Oblatt-Montal, M., and Montal, M. (1999) Structures of the M2 channel-lining segments from nicotinic acetylcholine and NMDA receptors by NMR spectroscopy. *Nat. Struct. Biol. 6*, 374–379.
11. Jones, D. H., Barber, K. R., VanDerLoo, E. W., and Grant, C. W. (1998) Epidermal growth factor receptor transmembrane domain: ^{2}H NMR implications for orientation and motion in a bilayer environment. *Biochemistry 37*, 16780–16787.
12. Smith, R., Separovic, F., Milne, T. J., Whittaker, A., Bennett, F. M., Cornell, B. A., and Makriyannis, A. (1994) Structure and orientation of the pore-forming peptide, melittin, in lipid bilayers. *J. Mol. Biol. 241*, 456–466.
13. Arkin, I. T. (2006) Isotope-edited IR spectroscopy for the study of membrane proteins. *Curr. Opin. Chem. Biol. 10*, 394–401.
14. Wu, Y., Huang, H. W., and Olah, G. A. (1990) Method of oriented circular dichroism. *Biophys. J. 57*, 797–806.
15. Bürck, J., Roth, S., Wadhwani, P., Afonin, S., Kanithasen, N., Strandberg, E., and Ulrich, A. S. (2008) Conformation and membrane orientation of amphiphilic helical peptides by oriented circular dichroism. *Biophys. J. 95*, 3872–3881.
16. Koehorst, R. B., Spruijt, R. B., Vergeldt, F. J., and Hemminga, M. A. (2004) Lipid bilayer topology of the transmembrane α-helix of M13 Major coat protein and bilayer polarity profile by site-directed fluorescence spectroscopy. *Biophys. J. 87*, 1445–1455.
17. Inbaraj, J. J., Cardon, T. B., Laryukhin, M., Grosser, S. M., and Lorigan, G. A. (2006) Determining the topology of integral membrane peptides using EPR spectroscopy. *J. Am. Chem. Soc. 128*, 9549–9554.
18. Jayasinghe, S., Hristova, K., and White, S. H. (2001) Energetics, stability, and prediction of transmembrane helices. *J. Mol. Biol. 312*, 927–934.
19. Kyte, J., and Doolittle, R. F. (1982) A simple method for displaying the hydropathic character of a protein. *J. Mol. Biol. 157*, 105–132.
20. Engelman, D. M., Steitz, T. A., and Goldman, A. (1986) Identifying nonpolar transbilayer helices in amino acid sequences of membrane proteins. *Annu. Rev. Biophys. Biophys. Chem. 15*, 321–353.
21. Eisenberg, D., Wilcox, W., and McLachlan, A. D. (1986) Hydrophobicity and amphiphilicity in protein structure. *J. Cell. Biochem. 31*, 11–17.
22. Bernsel, A., Viklund, H., Falk, J., Lindahl, E., von Heijne, G., and Elofsson, A. (2008) Prediction of membrane-protein topology from first principles. *Proc. Natl. Acad. Sci. U.S.A. 105*, 7177–7181.
23. Wimley, W. C., Creamer, T. P., and White, S. H. (1996) Solvation energies of amino acid side chains and backbone in a family of host-guest pentapeptides. *Biochemistry 35*, 5109–5124.
24. Guy, H. R. (1985) Amino acid side-chain partition energies and distribution of residues in soluble proteins. *Biophys. J. 47*, 61–70.
25. Radzicka, A., and Wolfenden, R. (1988) Comparing the polarities of the amino acids: Side-chain distribution coefficients between the

vapor phase, cyclohexane, 1-octanol, and neutral aqueous solution. *Biochemistry 27*, 1664–1670.
26. Wimley, W. C., and White, S. H. (1996) Experimentally determined hydrophobicity scale for proteins at membrane interfaces. *Nat. Struct. Biol. 3*, 842–848.
27. Hessa, T., Kim, H., Bihlmaier, K., Lundin, C., Boekel, J., Andersson, H., Nilsson, I., White, S. H., and Heijne, G. V. (2005) Recognition of transmembrane helices by the endoplasmic reticulum translocon. *Nature 433*, 377–381.
28. Senes, A., Chadi, D. C., Law, P. B., Walters, R. F. S., Nanda, V., and Degrado, W. F. (2007) E(z), a depth-dependent potential for assessing the energies of insertion of amino acid side-chains into membranes: Derivation and applications to determining the orientation of transmembrane and interfacial helices. *J. Mol. Biol. 366*, 436–448.
29. Ulmschneider, M. B., and Sansom, M. S. P. (2001) Amino acid distributions in integral membrane protein structures. *Biochim. Biophys. Acta 1512*, 1–14.
30. Johansson, A. C. V., and Lindahl, E. (2008) Position-resolved free energy of solvation for amino acids in lipid membranes from molecular dynamics simulations. *Proteins 70*, 1332–1344.
31. MacCallum, J. L., Bennett, W. F. D., and Tieleman, D. P. (2008) Distribution of amino acids in a lipid bilayer from computer simulations. *Biophys. J. 94*, 3393–3404.
32. Sengupta, D., Meinhold, L., Langosch, D., Ullmann, G. M., and Smith, J. C. (2005) Understanding the energetics of helical peptide orientation in membranes. *Proteins 58*, 913–922.
33. Sengupta, D., Smith, J. C., and Ullmann, G. M. (2008) Partitioning of amino-acid analogues in a five-slab membrane model. *Biochim. Biophys. Acta 1778*, 2234–2243.
34. Ulmschneider, M. B., Ulmschneider, J. P., Sansom, M. S. P., and Di Nola, A. (2007) A generalized Born implicit-membrane representation compared to experimental insertion free energies. *Biophys. J. 92*, 2338–2349.
35. Im, W., Feig, M., and Brooks, C. L.III (2003) An implicit membrane generalized born theory for the study of structure, stability, and interactions of membrane proteins. *Biophys. J. 85*, 2900–2918.
36. Kessel, A., Cafiso, D. S., and Ben-Tal, N. (2000) Continuum solvent model calculations of alamethicin-membrane interactions: Thermodynamic aspects. *Biophys. J. 78*, 571–583.
37. Mouritsen, O. G., and Bloom, M. (1984) Mattress model of lipid-protein interactions in membranes. *Biophys. J. 46*, 141–153.
38. Owicki, J. C., and McConnell, H. M. (1979) Theory of protein-lipid and protein-protein interactions in bilayer membranes. *Proc. Natl. Acad. Sci. U.S.A. 76*, 4750–4754.
39. Lomize, A. L., Pogozheva, I. D., Lomize, M. A., and Mosberg, H. I. (2006) Positioning of proteins in membranes: A computational approach. *Protein Sci. 15*, 1318–1333.
40. Ulmschneider, M. B., Sansom, M. S. P., and Di Nola, A. (2006) Evaluating tilt angles of membrane-associated helices: Comparison of computational and NMR techniques. *Biophys. J. 90*, 1650–1660.
41. Lomize, M. A., Lomize, A. L., Pogozheva, I. D., and Mosberg, H. I. (2006) OPM: Orientations of proteins in membranes database. *Bioinformatics 22*, 623–625.
42. Fares, C., Qian, J., and Davis, J. H. (2005) Magic angle spinning and static oriented sample NMR studies of the relaxation in the rotating frame of membrane peptides. *J. Chem. Phys. 122*, 194908.
43. Esteban-Martín, S., and Salgado, J. (2007) The dynamic orientation of membrane-bound peptides: Bridging simulations and experiments. *Biophys. J. 93*, 4278–4288.
44. Özdirekcan, S., Etchebest, C., Killian, J. A., and Fuchs, P. F. J. (2007) On the orientation of a designed transmembrane peptide: Toward the right tilt angle? *J. Am. Chem. Soc. 129*, 15174–15181.
45. Straus, S. K., Scott, W. R., and Watts, A. (2003) Assessing the effects of time and spatial averaging in ^{15}N chemical shift/^{15}N-^{1}H dipolar correlation solid state NMR experiments. *J. Biomol. NMR 26*, 283–295.
46. Shi, L., Cembran, A., Gao, J., and Veglia, G. (2009) Tilt and azimuthal angles of a transmembrane peptide: A comparison between molecular dynamics calculations and solid-state NMR data of sarcolipin in lipid membranes. *Biophys. J. 96*, 3648–3662.
47. Strandberg, E., Esteban-Martín, S., Salgado, J., and Ulrich, A. S. (2009) Orientation and dynamics of peptides in membranes calculated from ^{2}H-NMR data. *Biophys. J. 96*, 3223–3232.
48. Esteban-Martín, S., Strandberg, E., Fuertes, G., Ulrich, A. S., and Salgado, J. (2009) Influence of whole-body dynamics on ^{15}N PISEMA NMR spectra of membrane proteins: A theoretical analysis. *Biophys. J. 96*, 3233–3241.
49. Lindahl, E., and Sansom, M. S. P. (2008) Membrane proteins: Molecular dynamics simulations. *Curr. Opin. Struct. Biol 18*, 425–431.
50. Strandberg, E., Özdirekcan, S., Rijkers, D. T., Wel, P. C. V. D., Koeppe, R. E.II, Liskamp, R. M., and Killian, J. A. (2004) Tilt angles of transmembrane model peptides in oriented and non-oriented lipid bilayers as determined by ^{2}H solid-state NMR. *Biophys. J. 86*, 3709–3721.
51. van der Wel, P. C., Strandberg, E., Killian, J. A., and Koeppe, R. E.II (2002) Geometry and intrinsic tilt of a tryptophan-anchored transmembrane α-helix determined by ^{2}H NMR. *Biophys. J. 83*, 1479–1488.
52. Tremouilhac, P., Strandberg, E., Wadhwani, P., and Ulrich, A. S. (2006) Conditions affecting the re-alignment of the antimicrobial peptide PGLa in membranes as monitored by solid state ^{2}H-NMR. *Biochim. Biophys. Acta 1758*, 1330–1342.
53. Strandberg, E., Wadhwani, P., Tremouilhac, P., Durr, U. H., and Ulrich, A. S. (2006) Solid-state NMR analysis of the PGLa peptide orientation in DMPC bilayers: Structural fidelity of ^{2}H-labels versus high sensitivity of ^{19}F-NMR. *Biophys. J. 90*, 1676–1686.
54. Hristova, K., and White, S. H. (2005) An experiment-based algorithm for predicting the partitioning of unfolded peptides into phosphatidylcholine bilayer interfaces. *Biochemistry 44*, 12614–12619.
55. Pauls, K. P., MacKay, A. L., Söderman, O., Bloom, M., Tanjea, A. K., and Hodges, R. S. (1985) Dynamic properties of the backbone of an integral membrane polypeptide measured by ^{2}H-NMR. *Eur. Biophys. J. 12*, 1–11.
56. Schwede, T., Kopp, J., Guex, N., and Peitsch, M. C. (2003) SWISS-MODEL: An automated protein homology-modeling server. *Nucleic Acids Res. 31*, 3381–3385.
57. Im, W., and Brooks, C. L.III (2005) Interfacial folding and membrane insertion of designed peptides studied by molecular dynamics simulations. *Proc. Natl. Acad. Sci. U.S.A. 102*, 6771–6776.
58. Kucerka, N., Liu, Y., Chu, N., Petrache, H. I., Tristram-Nagle, S., and Nagle, J. F. (2005) Structure of fully hydrated fluid phase DMPC and DLPC lipid bilayers using X-ray scattering from oriented multilamellar arrays and from unilamellar vesicles. *Biophys. J. 88*, 2626–2637.
59. Nagle, J. F., and Tristram-Nagle, S. (2000) Structure of lipid bilayers. *Biochim. Biophys. Acta 1469*, 159–195.
60. de Planque, M. R. R., Greathouse, D. V., Koeppe, R. E.II, Schafer, H., Marsh, D., and Killian, J. A. (1998) Influence of lipid/peptide hydrophobic mismatch on the thickness of diacylphosphatidylcholine bilayers. A ^{2}H NMR and ESR study using designed transmembrane α-helical peptides and gramicidin A. *Biochemistry 37*, 9333–9345.
61. de Planque, M. R. R., Kruijtzer, J. A., Liskamp, R. M., Marsh, D., Greathouse, D. V., Koeppe, R. E.II, Kruijff, B. D., and Killian, J. A. (1999) Different membrane anchoring positions of tryptophan and lysine in synthetic transmembrane α-helical peptides. *J. Biol. Chem. 274*, 20839–20846.
62. White, S. H., and Wimley, W. C. (1999) Membrane protein folding and stability: Physical principles. *Annu. Rev. Biophys. Biomol. Struct. 28*, 319–365.
63. Hirota, N., Mizuno, K., and Goto, Y. (1998) Group additive contributions to the alcohol-induced α-helix formation of melittin: Implication for the mechanism of the alcohol effects on proteins. *J. Mol. Biol. 275*, 365–378.
64. Scarpelli, F., Drescher, M., Rutters-Meijneke, T., Holt, A., Rijkers, D. T. S., Killian, J. A., and Huber, M. (2009) Aggregation of Transmembrane Peptides Studied by Spin-Label EPR. *J. Phys. Chem. B 113*, 12257–12264.
65. Kandasamy, S. K., and Larson, R. G. (2006) Molecular dynamics simulations of model trans-membrane peptides in lipid bilayers: A systematic investigation of hydrophobic mismatch. *Biophys. J. 90*, 2326–2343.
66. Prosser, R. S., Daleman, S. I., and Davis, J. H. (1994) The structure of an integral membrane peptide: A deuterium NMR study of gramicidin. *Biophys. J. 66*, 1415–1428.
67. Davis, J. H., Auger, M., and Hodges, R. S. (1995) High resolution ^{1}H nuclear magnetic resonance of a transmembrane peptide. *Biophys. J. 69*, 1917–1932.
68. Marrink, S. J., Risselada, H. J., Yefimov, S., Tieleman, D. P., and de Vries, A. H. (2007) The MARTINI force field: Coarse grained model for biomolecular simulations. *J. Phys. Chem. B 111*, 7812–7824.